Density Functional Theory for Strongly-Interacting Electrons

Francesc Malet, André Mirtschink, Klaas J. H. Giesbertz and Paola Gori-Giorgi

Abstract Although *Kohn–Sham* (KS) density functional theory (DFT) is an exact theory, able in principle to describe any interacting N-electron system in terms of the non-interacting Kohn–Sham model, in practice only approximate expressions for the exchange-correlation term are available. For decades, a large number of such approximations have been developed, proving enormously successful and accurate for applications in many different fields. However, there still remain important situations, of both fundamental and practical interest, for which all the commonly employed exchange-correlation functionals fail to provide an accurate description. The paradigm of such scenarios are those systems in which the electronic correlation plays the most important role. In this chapter, we show how the knowledge on the strong-interaction limit of DFT, recently formulated within the so-called *strictly-correlated-electrons* (SCE) formalism, can be imported into the Kohn–Sham approach and used to build approximations for the exchange-correlation energy that are able to reproduce key features of the strongly-correlated regime. We report results of the first applications of this "*KS SCE*" DFT approach on quasi-one-dimensional systems, showing its very good accuracy in the limits of both vanishing and infinite correlation. In the last part of the chapter, we propose a generalization of the approach for its application to more general systems.

F. Malet · A. Mirtschink · K. J. H. Giesbertz · P. Gori-Giorgi (✉)
Department of Theoretical Chemistry—Faculty of Sciences, Vrije Universiteit Amsterdam, De Boelelaan 1083, 1081 HV Amsterdam, The Netherlands
e-mail: p.gorigiorgi@vu.nl

F. Malet
e-mail: f.maletgiralt@vu.nl

A. Mirtschink
e-mail: a.p.mirtschink@vu.nl

K. J. H. Giesbertz
e-mail: k.j.h.giesbertz@vu.nl

V. Bach and L. Delle Site (eds.), *Many-Electron Approaches in Physics, Chemistry and Mathematics*, Mathematical Physics Studies, DOI: 10.1007/978-3-319-06379-9_8,

1 Introduction

The key idea of Kohn–Sham (KS) density functional theory (DFT) is an exact mapping [1] between the physical, interacting, many-electron system and a model system of non-interacting fermions with the same density, allowing for a realistic treatment of the electronic kinetic energy. All the complicated many-body effects are embedded in the so-called exchange-correlation (xc) energy functional. Although, in principle, the exact xc functional exists and is unique (and "universal"), in practice it needs to be approximated. Both physicists and chemists have developed a large number of approximations in the last twenty years, often targeting different systems, different properties, and different phenomena (see in particular Chap. "Computational Techniques for Density Functional-based Molecular Dynamics Calculations in Plane-Wave and Localized Basis Sets" by Tzanov and Tuckermann, "Application of (Kohn–Sham) Density Functional Theory to Real Materials" by Ghiringhelli, von Lilienfeld and Karasiev et al.)

Despite all these efforts, there are still important cases in which state-of-the-art KS DFT fails, which is why the quest for better xc functionals continues to be a very active research field [2–4]. For example [3, 5], present-day KS DFT encounters severe problems in the treatment of near-degeneracy and strong-correlation effects (rearrangement of electrons within partially filled levels, important for describing not only bond dissociation but also equilibrium geometries, particularly for systems with d and f unsaturated shells, such as transition metals and actinides, Mott insulators, and low-density nanodevices—see also Chap. "Electronic Structure Calculations with LDA + DMFT" by Pavarini) and in the description of van der Waals long-range interactions (relevant, for example, for biomolecules and layered materials—see also Chap. "Linear Response Methods in Quantum Chemistry" by Watermann et al.). While on this latter issue there has been considerable progress in the last years through long-range energy corrections, the difficulties related to near degeneracy and strong correlation are certainly the most important open problem of KS DFT (and of many-body quantum physics in general). These difficulties can hamper more or less severely (and sometimes in an unpredictable way) a given calculation, depending on their relative importance with respect to other effects that are better captured by the available approximate functionals.

Both in Physics and Chemistry, strong electronic correlation is often mimicked by the approximate functionals with spin and spatial symmetry breaking, which, however, leads to several problems. For example, for transition metal complexes symmetry breaking occurs erratically, and is very sensitive to the functional chosen. The consequences are wrong characterizations of the ground and excited states, and problems in keeping the potential energy surfaces continuous.

The aim of this chapter is to introduce a novel approach to treat systems in which the electron–electron interaction plays a prominent role within KS DFT without using symmetry breaking, and to summarize some results. The approach is based on the exact strong-interaction limit of DFT [6–8], described by the so-called "strictly-correlated-electrons" (SCE) functional. The SCE functional defines a problem that

is neither purely classical nor quantum mechanical. It can be reformulated [9] in the language of optimal transport (or mass transportation theory), an important field of mathematics and economics. This reformulation is also illustrated and discussed.

2 Combining the Kohn–Sham and the Strictly-Correlated-Electrons Functional

2.1 Kohn–Sham DFT

For a system of N interacting electrons in an external potential $v_{\text{ext}}(\mathbf{r})$, the total energy can be written as a functional of the density given by [10]

$$E[\rho] = F[\rho] + \int d\mathbf{r}\, v_{\text{ext}}(\mathbf{r})\, \rho(\mathbf{r}) \,, \tag{1}$$

where $F[\rho]$ is the universal Hohenberg-Kohn functional, defined as the minimum of the sum of the kinetic energy $\hat{T}$ and the electron–electron repulsion $\hat{V}_{ee}$ with respect to all the fermionic wave functions Ψ that yield the density $\rho(\mathbf{r})$ [11] (see also Chap. "Levy-Lieb Principle Meets Quantum Monte Carlo" Delle Site):

$$F[\rho] = \min_{\Psi \to \rho} \langle \Psi | \hat{T} + \hat{V}_{ee} | \Psi \rangle \,. \tag{2}$$

The ground-state energy of the system E_0 can be obtained variationally, and it is reached at the ground-state density $\rho_0(\mathbf{r})$, $E_0 = E[\rho = \rho_0]$.

Unfortunately, the exact explicit form of $F[\rho]$ is not known, and one must therefore build approximations for it. In *Kohn–Sham DFT*, this is done by introducing a reference system of non-interacting electrons with the same density as the physical, interacting one, and for which the kinetic energy can be exactly written as

$$T_s[\rho] = \min_{\Psi \to \rho} \langle \Psi | \hat{T} | \Psi \rangle = -\frac{1}{2} \sum_{i=1}^{N} \langle \phi_i | \nabla^2 | \phi_i \rangle \,, \tag{3}$$

where the ϕ_i are the so-called Kohn–Sham orbitals in terms of which the density is given as $\rho(\mathbf{r}) = \sum_i |\phi_i(\mathbf{r})|^2$, with the sum running over the occupied orbitals. The Hohenberg-Kohn functional is then partioned as

$$F[\rho] \equiv T_s[\rho] + E_{Hxc}[\rho] \equiv T_s[\rho] + E_H[\rho] + E_{xc}[\rho] \,, \tag{4}$$

where the last two terms define, respectively, the Hartree and the exchange-correlation functionals. The functional derivatives with respect to the density yield the Hartree and exchange-correlation potentials,

$$v_{\mathrm{H}}[\rho](\mathbf{r}) \equiv \frac{\delta E_{\mathrm{H}}[\rho]}{\delta\rho(\mathbf{r})}, \quad v_{\mathrm{xc}}[\rho](\mathbf{r}) \equiv \frac{\delta E_{\mathrm{xc}}[\rho]}{\delta\rho(\mathbf{r})}\,. \tag{5}$$

Since the Hartree contribution can be also calculated exactly, all the unknown information is contained in the exchange-correlation term, which must therefore be approximated. Once this is done in a suitable way, from the combination of the variational condition and Eqs. (3)–(5), one obtains the well-known Kohn–Sham equations:

$$\left(-\frac{1}{2}\nabla^2 + v_{\mathrm{KS}}[\rho](\mathbf{r})\right)\phi_i(\mathbf{r}) = \varepsilon_i\phi_i(\mathbf{r})\,, \tag{6}$$

where $v_{\mathrm{KS}}[\rho](\mathbf{r}) \equiv v_{\mathrm{H}}[\rho](\mathbf{r}) + v_{\mathrm{xc}}[\rho](\mathbf{r}) + v_{\mathrm{ext}}(\mathbf{r})$ defines the Kohn–Sham potential. Since $v_{\mathrm{KS}}[\rho](\mathbf{r})$ is density-dependent, Eq. (6) must be solved self-consistently.

2.2 Strictly-Correlated-Electrons Functional

Instead of discussing the commonly employed approximations for $E_{xc}[\rho]$ and their success and failures (for recent reviews, see, e.g., [4, 5]; in particular in this book see the Chap. "Application of (Kohn–Sham) Density Functional Theory to Real Materials" by Ghiringhelli), we focus here on the use of the exact strong-interaction limit of DFT in the KS formalism.

The HK functional of Eq. (2) and the KS functional of Eq. (3) can be seen as the values at $\lambda = 1$ and $\lambda = 0$ of a more general functional $F_\lambda[\rho]$, in which the electron–electron interaction strength is rescaled with a real parameter λ,

$$F_\lambda[\rho] = \min_{\Psi\to\rho} \langle\Psi|\hat{T} + \lambda\hat{V}_{ee}|\Psi\rangle. \tag{7}$$

A well-known exact formula for $E_{\mathrm{Hxc}}[\rho]$ is [12, 13]

$$E_{\mathrm{Hxc}}[\rho] = \int_0^1 \langle\Psi_\lambda[\rho]|V_{ee}|\Psi_\lambda[\rho]\rangle\, d\lambda \equiv \int_0^1 V_{ee}^{\lambda}[\rho]\, d\lambda, \tag{8}$$

where $\Psi_\lambda[\rho]$ is the minimizing wave function in Eq. (7). The SCE functional corresponds to the leading term in the $\lambda \to \infty$ expansion of the integrand in Eq. (8) [6–8, 14, 15],

$$V_{ee}^{\lambda\to\infty}[\rho] = V_{ee}^{\mathrm{SCE}}[\rho] + O(\lambda^{-1/2}). \tag{9}$$

By inserting Eq. (9) into Eq. (8), we obtain a zeroth-order expansion at $\lambda = \infty$ for $E_{\mathrm{Hxc}}[\rho]$,

$$E_{\mathrm{Hxc}}[\rho] \approx V_{ee}^{\mathrm{SCE}}[\rho]. \tag{10}$$

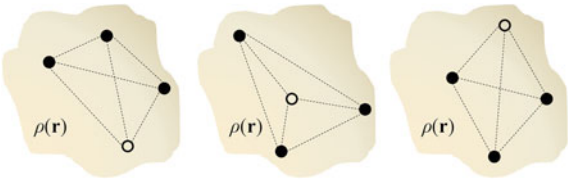

Fig. 1 Schematic illustration of the SCE reference system for a given density $\rho(\mathbf{r})$ and $N = 4$ electrons. The *empty circle* represents the position of the reference particle in each case. The SCE state is a superposition of an infinite number of these configurations, one for each value of the position of the reference electron $\mathbf{r}$. This infinite superposition keeps the density of the system equal to $\rho(\mathbf{r})$

The functional $V_{ee}^{\mathrm{SCE}}[\rho]$ corresponds to the minimization of the electronic interaction alone over all wave functions yielding the given density ρ,

$$V_{ee}^{\mathrm{SCE}}[\rho] = \min_{\Psi\to\rho} \langle \Psi | \hat{V}_{ee} | \Psi \rangle. \tag{11}$$

Equation (10) is thus equivalent to approximate the constrained minimization over Ψ in the HK functional of Eq. (2) with the sum of the two constrained minima [16, 17]:

$$F[\rho] \approx \min_{\Psi\to\rho} \langle \Psi | \hat{T} | \Psi \rangle + \min_{\Psi\to\rho} \langle \Psi | \hat{V}_{ee} | \Psi \rangle \equiv T_s[\rho] + V_{ee}^{\mathrm{SCE}}[\rho]\ . \tag{12}$$

The functional $V_{ee}^{\mathrm{SCE}}[\rho]$ was introduced by Seidl and co-workers in the SCE formulation of DFT [6–8, 18]. They showed that it corresponds to the electron–electron interaction of a fictitious system, with density $\rho(\mathbf{r})$, and in which the electrons are infinitely correlated and have zero kinetic energy.

For a more rigorous derivation, we refer the reader to [7], while here we only aim at sketching the physics behind the SCE functional. In the SCE system, which appears clearly as the natural counterpart of the non-interacting Kohn–Sham one, the electrons can be seen as classical point charges located at the lattice sites of a "floating" Wigner crystal. This means that if one electron (which is taken as reference) is at a certain position $\mathbf{r}$, due to the infinite correlation the crystal must deform itself adjusting the positions of the other $N-1$ electrons in order to keep the density equal to $\rho(\mathbf{r})$ at each point of space. As schematically represented in Fig. 1, the SCE reference system corresponds to a superposition of an infinite number of configurations (one for each value of the reference position $\mathbf{r}$).

Since the positions of the remaining $N-1$ electrons become a function of the position $\mathbf{r}$ of the reference one, they are represented with the so-called *co-motion functions* $\mathbf{f}_i(\mathbf{r})$ $(i = 1, \ldots, N)$, with $\mathbf{f}_1(\mathbf{r}) \equiv \mathbf{r}$ if we take, e.g., the electron "1" as a reference. For a given density $\rho(\mathbf{r})$, the probability of finding this electron at $\mathbf{r}$ will therefore be the same as that of finding the electron "i" at $\mathbf{f}_i(\mathbf{r})$, i.e.,

$$\rho(\mathbf{f}_i(\mathbf{r}))d\mathbf{f}_i(\mathbf{r}) = \rho(\mathbf{r})d\mathbf{r}\ . \tag{13}$$

Equation (13) is one of the fundamental relations in SCE DFT, showing that, in principle, for a given density one can obtain the co-motion functions by integration. Notice that the co-motion functions must satisfy the following cyclic group properties, in order to ensure the indistinguishability of the electrons [7],

$$\begin{aligned}
&\mathbf{f}_1(\mathbf{r}) \equiv \mathbf{r},\\
&\mathbf{f}_2(\mathbf{r}) \equiv \mathbf{f}(\mathbf{r}),\\
&\mathbf{f}_3(\mathbf{r}) = \mathbf{f}(\mathbf{f}(\mathbf{r})),\\
&\mathbf{f}_4(\mathbf{r}) = \mathbf{f}(\mathbf{f}(\mathbf{f}(\mathbf{r})),\\
&\qquad\vdots\\
&\underbrace{\mathbf{f}(\mathbf{f}(\ldots\mathbf{f}(\mathbf{f}(\mathbf{r}))}_{N\text{ times}} = \mathbf{r}.
\end{aligned} \tag{14}$$

In terms of the co-motion functions the SCE functional is then equal to

$$V_{ee}^{\mathrm{SCE}}[\rho] = \int d\mathbf{s}\frac{\rho(\mathbf{s})}{N}\sum_{i=1}^{N-1}\sum_{j=i+1}^{N}\frac{1}{|\mathbf{f}_i(\mathbf{s}) - \mathbf{f}_j(\mathbf{s})|} = \frac{1}{2}\int d\mathbf{s}\,\rho(\mathbf{s})\sum_{i=2}^{N}\frac{1}{|\mathbf{s} - \mathbf{f}_i(\mathbf{s})|}, \tag{15}$$

just as $T_s[\rho]$ is written in terms of the Kohn–Sham orbitals $\phi_i(\mathbf{r})$. The equivalence of the two expressions for $V_{ee}^{\mathrm{SCE}}[\rho]$ in Eq. (15) has been proven in Ref. [19].

Another important consequence of the properties of the SCE reference system is that the net Coulomb repulsion felt by an electron at position $\mathbf{r}$, depending on the positions of the other particles, becomes a function of $\mathbf{r}$ itself. This force can therefore be written as minus the gradient of some *local one-body potential* [7–9]:

$$-\nabla v_{\mathrm{SCE}}[\rho](\mathbf{r}) \equiv \mathbf{F}_{\mathrm{Coulomb}}(\mathbf{r}) = \sum_{i=2}^{N}\frac{\mathbf{r} - \mathbf{f}_i[\rho](\mathbf{r})}{|\mathbf{r} - \mathbf{f}_i[\rho](\mathbf{r})|^3}\ . \tag{16}$$

Finally, it can be easily shown that this one-body potential satisfies in turn the exact relation with the SCE functional [17, 18]

$$v_{\mathrm{SCE}}[\rho](\mathbf{r}) = \frac{\delta V_{ee}^{\mathrm{SCE}}[\rho(\mathbf{r})]}{\delta\rho(\mathbf{r})}\ . \tag{17}$$

Taking the functional derivatives in Eq. (12), we then see that the approximation of Eq. (12) corresponds in modeling the Hartree and exchange-correlation potential with $v_{\mathrm{SCE}}[\rho](\mathbf{r})$,

$$v_{\mathrm{H}}(\mathbf{r}) + v_{\mathrm{xc}}(\mathbf{r}) \approx v_{\mathrm{SCE}}(\mathbf{r})\ . \tag{18}$$

To perform practical calculations, one must proceed self-consistently in three steps: (i) integrate Eq. (13) for a given density $\rho(\mathbf{r})$ in order to obtain the co-motion functions; (ii) compute the sum in the right-hand-side of Eq. (16) and calculate $v_{\rm SCE}$ by integration; (iii) use the approximation of Eq. (18) to solve the Kohn–Sham equations (6). The total energy is then obtained from Eqs. (1) and (12). At the end of the chapter we discuss the inclusion of corrections to the approximation made in Eq. (10). In the next section, we illustrate this method for calculations in (quasi) one-dimensional systems.

3 Applications to Quasi-One-Dimensional Systems

We report here some results obtained from the first applications of the zeroth-order KS SCE approach to two different kinds of one-dimensional systems: semiconductor quantum wires with harmonic confinement and artificial hydrogen atoms with soft-Coulomb interaction. The results are compared with those obtained with the Configuration Interaction (CI) approach and with the local density approximation (LDA, [20, 21]) of standard Kohn–Sham DFT. All the KS SCE and KS LDA calculations have been performed within the spin-restricted framework, in which each spatial orbital is doubly occupied.

In one dimension, the co-motion functions can be easily obtained by integrating Eq. (13) for a given density $\rho(x)$ [6, 9, 22] imposing boundary conditions that make the density between two adjacent strictly-correlated positions always integrate to 1:

$$\int_{f_i(x)}^{f_{i+1}(x)} \rho(x')\,dx' = 1\ , \tag{19}$$

and ensuring that the $f_i(x)$ satisfy the group properties of Eq. (14) [6, 7]. One then obtains

$$f_i(x) = \begin{cases} N_e^{-1}[N_e(x) + i - 1] & x \le N_e^{-1}(N + 1 - i) \\ N_e^{-1}[N_e(x) + i - 1 - N] & x > N_e^{-1}(N + 1 - i), \end{cases} \tag{20}$$

where the monotonic increasing function $N_e(x)$ is defined as

$$N_e(x) = \int_{-\infty}^{x} \rho(x')\,dx', \tag{21}$$

and $N_e^{-1}(x)$ is its inverse. Notice that the SCE functional is a highly non-local density functional, containing as main ingredient the integral of the density, $N_e(x)$ of Eq. (21). This is very different than the commonly used approximations (LDA,

generalized gradient approximations, etc.) that depend only locally or semi-locally on the density.

3.1 Quantum Wires

We have considered first N electrons in a (quasi-)one-dimensional quantum wire in which the effective electron–electron interaction $w_b(x)$ is obtained by integrating the Coulomb repulsion on the lateral degrees of freedom [23, 25],

$$w_b(x) = \frac{\sqrt{\pi}}{2\,b}\,\exp\left(\frac{x^2}{4\,b^2}\right)\mathrm{erfc}\left(\frac{x}{2\,b}\right). \tag{22}$$

The parameter b in Eq. (22) fixes the thickness of the wire (here set equal to $b = 0.1$) and $\mathrm{erfc}(x)$ is the complementary error function. The interaction $w_b(x)$ has a long-range coulombic tail, $w_b(x \to \infty) = 1/x$, and is finite at the origin, where it has a cusp. We also consider an harmonic confinement in the direction of motion of the electrons, $v_{\mathrm{ext}} = \omega^2 x^2/2$, where $\omega \equiv 4/L^2$ is the confinement frequency in terms of the effective length of the wire L [23, 24]. As L increases, the interactions become dominant and the system enters the strongly correlated regime, characterized by charge density localization.

The left panel in Fig. 2 shows the electron densities for $N = 4$ electrons and different effective confinement lengths L. One can see that when the wire has a short effective length, here represented by $L = 1$, the electrons are weakly correlated and the three approaches show a very good agreement. The density displays $N/2$ peaks, given by the Friedel-like oscillations with wave number $2k_F^{\mathrm{eff}}$, where $k_F^{\mathrm{eff}} = \pi\tilde{\rho}/2$ is the effective Fermi wavenumber. When the effective length of the wire increases, the electronic correlation begins to play a dominant role in the system. This corresponds to $L = 15$, where one can see that while the CI density starts to develop a 4-peak structure, corresponding to an incipient charge density localization, the LDA yields a qualitatively wrong description of the system, with a density that becomes very delocalized along the wire. In contrast, although not being quantitatively very accurate, the $2k_F \to 4k_F$ crossover is clearly qualitatively well-captured by the KS SCE approach. Finally, for a long wire ($L = 70$), the agreement between the KS SCE and CI results improves significantly, now both displaying four very clearly marked peaks in the density, whereas the LDA result becomes completely inaccurate, with a density that is almost flat in the scale of the figure.

The failure of the KS LDA approach in the intermediate and strong correlation regimes is representative of all the approximate functionals, including generalized gradient approximations (GGA), exact-exchange and self-interaction corrections (SIC), which never succeeded in reproducing the peak splitting in the electronic density without introducing an artificial magnetic order [26, 27].

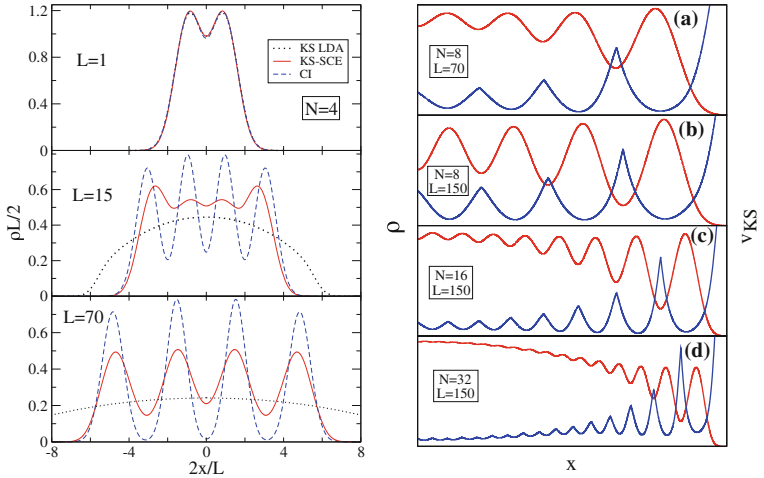

Fig. 2 *Left panel* one-electron densities obtained with the KS SCE, CI and KS LDA approaches for the $N = 4$ model quantum wire in the weak ($L = 1$), intermediate ($L = 15$) and strong ($L = 70$) correlation regime. *Right panel* one electron densities (*red*) and corresponding Kohn–Sham potentials (*blue*) obtained from the self-consistent KS SCE approach for model quantum wires with different numbers of electrons N in different regimes of correlation (for clarity, only the part $x > 0$ is shown)

It is known that the exact v_{KS} must build "bumps" or barriers in order to separate the electrons when the latter localize [28, 29]. In the right panel of the same Fig. 2 we show the self-consistent Kohn–Sham potentials and densities corresponding to the KS SCE approach for wires with different number of electrons N and effective confinement lengths L. One can see that the KS SCE potential displays $N - 1$ "bumps", each of them corresponding to a local minimum in the density. It must be stressed that none of the commonly employed approximations in spin-restricted Kohn–Sham DFT is able to reproduce this key feature of the exact KS potential. Regarding total energies, the KS SCE approach has a relative accuracy of about 2–3 % at $L = 70$ [17]. This accuracy increases as L increases.

Finally, we also want to point out the cheap computational cost of the KS SCE approach in one dimension. Indeed, while the numerical effort involved in the CI method increases exponentially with the number of particles, especially in the strong-correlation regime that requires very large Hilbert spaces, in the KS SCE case it becomes similar to that associated with the usual KS LDA. For example, the data in the right panel of Fig. 2 have been obtained in a few minutes on a desktop computer.

3.2 *Model* H_2 *Molecule*

The implementation of the SCE functional in the three-dimensional (3D) space has been achieved, so far, only for spherically symmetric systems. For general 3D geometry we discuss in Sect. 5 an alternative formulation which does not need the knowledge of the co-motion functions. In this section, instead, we explore the performance of the SCE functional for 1D models in chemistry [21, 30], focussing on the breaking of the chemical bond, which is one of the biggest open problems in spin-restricted Kohn–Sham calculations [3, 31].

Following Refs. [21, 32], we consider a 1D model for the H_2 molecule in which the nuclei are separated by a variable distance R_{H-H} and the electron–electron and nuclei-electron interactions are modeled with a soft-coulomb potential given by

$$v_{ee}(x) = -v_{ne}(x) = \frac{1}{\sqrt{1+x^2}} \,. \tag{23}$$

Figure 3 shows the total energies of the H_2 molecule as a function of the interatomic separation R_{H-H}, obtained with the KS SCE, CI and KS LDA approaches, in a spin-restricted formalism (that is, without localizing the spin densities on each atom). We also show the result with restricted Hartree–Fock (HF). It can be seen that while KS LDA shows a very good agreement with the exact result at equilibrium, a large error is made by the KS SCE approach, which yields a much lower energy due to its overestimation of the correlation. Yet, the equilibrium distance predicted by the KS SCE approach is not too different from the exact one. As the interatomic distance increases, however, the LDA energy rapidly deviates from the CI result, becoming too positive, similarly to the well-known three-dimensional case. Contrarily, the KS SCE result becomes now increasingly more accurate, reaching the exact curve in the dissociation limit. Again, this feature is out of reach for all the existing approximations in restricted Kohn–Sham DFT.

In order to improve the accuracy of the KS SCE approach at small interatomic separations, one could include corrections to the zeroth-order approximation of Eq. (4), which we briefly discuss in the next section. As a first test, we have calculated, at a post-functional level, the first-order correction to the KS SCE results, which we also show in the same Fig. 3. It can be seen that this correction significantly improves the KS SCE energy curve at small interatomic distances, although it introduces some error on the equilibrium position. Also, it slightly shifts upwards the curve in the dissociation region, although with a much smaller error than the one made by the LDA. One could expect, however, that the implementation of the correction within the self-consistent procedure should provide more accurate results.

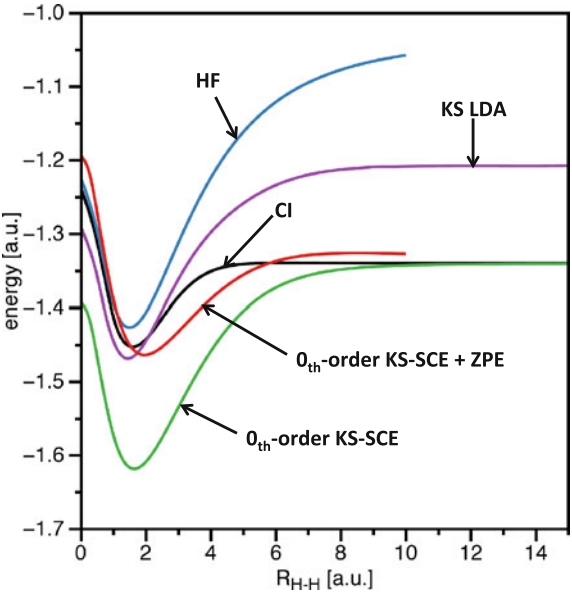

Fig. 3 Total energy of the 1D H_2 molecule as a function of the interatomic separation R_{H-H} corresponding to the HF, CI, KS LDA and KS SCE approaches. The result of including a post-functional first-order correction to the zeroth-order KS SCE approach is also shown

4 Corrections to the Zeroth-Order KS SCE Approach

In this section we discuss how to improve the zeroth-order KS SCE approach. In general, one can decompose $F[\rho]$ as

$$F[\rho] = T_s[\rho] + V_{ee}^{\mathrm{SCE}}[\rho] + T_c[\rho] + V_{ee}^{d}[\rho], \tag{24}$$

where $T_c[\rho]$ (kinetic correlation energy) is

$$T_c[\rho] = \langle \Psi[\rho] | \hat{T} | \Psi[\rho] \rangle - T_s[\rho], \tag{25}$$

i.e., the difference between the true kinetic energy and the Kohn–Sham one of Eq. (3), and $V_{ee}^{d}[\rho]$ (electron–electron decorrelation energy) is

$$V_{ee}^{d}[\rho] = \langle \Psi[\rho] | \hat{V}_{ee} | \Psi[\rho] \rangle - V_{ee}^{\mathrm{SCE}}[\rho], \tag{26}$$

i.e., the difference between the true expectation of $\hat{V}_{ee}$ and the SCE value.

4.1 Zero-Point Oscillations in the SCE System

A "first-order" approximation for $T_c[\rho] + V_{ee}^d[\rho]$ can be obtained by considering the next leading term in the $\lambda \to \infty$ expansion of Eq. (9),

$$V_{ee}^{\lambda\to\infty}[\rho] = V_{ee}^{\mathrm{SCE}}[\rho] + \frac{V_{ee}^{\mathrm{ZPE}}[\rho]}{\sqrt{\lambda}} + O(\lambda^{-p}), \tag{27}$$

where the acronym "ZPE" refers to "zero-point energy", and $p \geq 5/4$—see Ref. [8] for further details. This yields

$$T_c[\rho] + V_{ee}^d[\rho] \approx 2\, V_{ee}^{\mathrm{ZPE}}[\rho]. \tag{28}$$

Physically, the zeroth-order term $V_{ee}^{\mathrm{SCE}}[\rho]$ in the expansion (27) corresponds to the interaction energy when the electrons are "frozen" in the lattice sites of the SCE floating Wigner crystal. The ZPE term in the series takes into account small vibrations of the electrons around their positions, and it is given by [8]

$$V_{ee}^{\mathrm{ZPE}}[\rho] = \frac{1}{2}\int d\mathbf{r}\frac{\rho(\mathbf{r})}{N}\sum_{n=1}^{3N-3}\frac{\omega_n(\mathbf{r})}{2}\,. \tag{29}$$

The $\omega_n(\mathbf{r})$ are the zero-point-energy vibrational frequencies around the SCE minimum [8], given by the eigenvalues of the Hessian matrix entering the expansion up to second order of the potential energy of the electrons in the SCE system. We have included the electron–electron interaction part, Eq. (29), of the ZPE at the postfunctional level (that is, non self-consistently) to obtain the red curve in Fig. 3.

4.2 Corrections from Available approximate Functionals

It is also possible to extract approximations for $T_c[\rho] + V_{ee}^d[\rho]$ from available approximate functionals $E_{xc}^{\mathrm{approx}}[\rho]$. This can be done by using the scaling properties [33, 34] of DFT. By defining, for electrons in D dimensions, a scaled density $\rho_\gamma(\mathbf{r}) \equiv \gamma^D \rho(\gamma\,\mathbf{r})$ with $\gamma > 0$, we have [34]

$$T_c[\rho] + V_{ee}^d[\rho] \approx E_{xc}^{\mathrm{approx}}[\rho] - \lim_{\gamma\to 0}\frac{1}{\gamma}E_{xc}^{\mathrm{approx}}[\rho_\gamma]. \tag{30}$$

This way of constructing corrections to KS SCE has been only tested by using the LDA functional in Ref. [17] with rather disappointing results. However, much better results should be obtained with a metaGGA functional such as the one of Ref. [35], which can recognize one-electron regions important in the strongly-correlated limit.

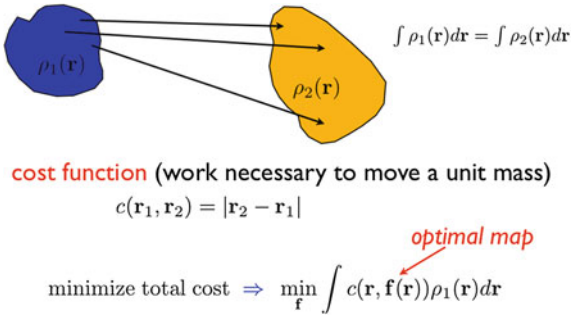

Fig. 4 The Monge problem of finding the most economical way of moving a mass distribution into another one. Usually, the work necessary to move a unit mass from one location to another is set equal to the distance between the two locations. The SCE functional defines a similar problem in which, instead, the cost function is given by the Coulomb repulsion, and the goal is to transport $N - 1$ times the density into itself

5 Optimal-Transport Reformulation of the SCE Functional

The exact SCE functional of Eq. (11) defines a problem that is neither properly classical (classical systems at zero temperature do not have smooth densities) nor quantum mechanical (there is zero kinetic energy, so that quantum effects do not enter). Notice that this does not imply that we do not take into account quantum effects: they enter when we use the SCE functional in the KS approach.

A very useful mathematical framework for the SCE functional is optimal transport (or mass transportation theory), an important field of mathematics and economics [9, 36]. Mass transportation theory dates back to 1781 when Monge [37] posed the problem of finding the most economical way of moving soil from one area to another, and received a boost when Kantorovich, in 1942, generalized it to what is now known as the Kantorovich dual problem [38]. In the last twenty years optimal transport has developed into one of the most fertile and active fields in mathematics, because long-standing issues could be finally addressed, and also because connections with classical problems in geometry, partial differential equations, nonlinear dynamics, and other problems of economics have been established [39].

The original Monge-Kantorovich problem consists in finding the most economical way to move a mass distribution into another one (according to a given definition of the cost function, which gives the work necessary to move a unit mass from one location to another). For example, one may wish to move books from one shelf ("shelf 1") to another ("shelf 2"), by minimizing the total work. The goal of solving the Monge problem is then to find an optimal map which assigns to every book in shelf 1 a unique final destination in shelf 2 (see Fig. 4).

In Ref. [9] it has been shown that the co-motion functions of the SCE theory are exactly the Monge optimal maps for a mass transportation problem with cost function given by the Coulomb repulsion. However, it is well known in mass transportation

theory that the Monge problem is very delicate and that proving in general the existence of the optimal maps (or co-motion functions) is extremely difficult. In 1942 Kantorovich proposed a relaxed formulation of the Monge problem, in which the goal is now to find a transport plan, which gives the probability that, when minimizing the total cost, a certain mass element in the first mass distribution be transported into another one in the second mass distribution. This is evidently more general than the Monge transportation map, which assigns a unique final destination in the second mass distribution to every element in the first one. It turns out [9] that the relaxed Kantorovich formulation is the appropriate one for the SCE problem. This way, it is possible to reformulate $V_{ee}^{\mathrm{SCE}}[\rho]$ as the maximum of the Kantorovich dual problem,

$$V_{ee}^{\mathrm{SCE}}[\rho] = \max_{u} \left\{ \int u(\mathbf{r})\rho(\mathbf{r})d\mathbf{r} \ : \ \sum_{i=1}^{N} u(\mathbf{r}_i) \leq \sum_{i=1}^{N-1} \sum_{j>i}^{N} \frac{1}{|\mathbf{r}_i - \mathbf{r}_j|} \right\},$$

where $u(\mathbf{r}) = v_{\mathrm{SCE}}[\rho](\mathbf{r}) + C$, and C is a constant [9]. The above expression corresponds to a maximization under linear constraints and yields, in one shot, the functional and its functional derivative. Since the latter is the one-body potential given by Eq. (17), used to approximate the Hartree-exchange-correlation term in KS SCE DFT, this reformulation allows one to obtain directly the potential without having to previously calculate the co-motion functions via Eq. (13).

Although the number of linear constraints is infinite, this formulation may indeed lead to approximate, but accurate, approaches to the construction of $V_{ee}^{\mathrm{SCE}}[\rho]$ and $v_{\mathrm{SCE}}[\rho](\mathbf{r})$, as very recently shown by the first pilot implementation of Mendl and Lin [40].

6 Conclusions and Perspectives

The knowledge on the strong-interaction limit of density functional theory can be used to construct approximations for the exchange-correlation energy and potential of Kohn–Sham DFT. Even at the lowest-order of approximation, this approach yields good results for both weakly- and strongly-interacting systems, without the need of introducing any artificial symmetry breaking. In particular, it is able to reproduce quantitatively key features of the strongly-correlated regime out of the reach of all the commonly employed approximations, such as the presence of "bumps" in the Kohn–Sham potential, responsible for, e.g., charge density localization in semiconductor nanostructures. At the same time, at least in one dimension, the computational cost of this approach is comparable to the one of standard KS LDA, way much cheaper than demanding wave function methods that are often the only route to treat strong correlation. This allows to treat systems with much larger number of particles and in arbitrary regimes of correlation.

In this chapter we have reported the first pilot applications of this approach on two simple one-dimensional systems, namely semiconductor quantum wires and a model for the hydrogen molecule. We have also discussed the inclusion of corrections in order to further improve the results obtained with the zeroth-order approach. Whereas only some minor modifications are needed in order to apply the formalism to systems with spherical symmetry, a generalization to arbitrary systems seems to be a much more complicated task. In this regard, it has recently been shown that a reformulation of the approach in terms of optimal transport theory, a well established field of mathematics, could be a successful route towards this goal.

Acknowledgments This work was supported by the Netherlands Organization for Scientific Research (NWO) through a Vidi grant (PG-G) and a Veni grant (KJHG), and by a Marie Curie Intra-European fellowship within the 7th European Community Framework Programme (FM).

References

1. Kohn, W., Sham, L.J.: Phys. Rev. A **140**, 1133 (1965)
2. Perdew, J.P., Ruzsinszky, A., Tao, J., Staroverov, V.N., Scuseria, G.E., Csonka, G.I.: J. Chem. Phys. **123**, 062201 (2005)
3. Cohen, A.J., Mori-Sanchez, P., Yang, W.T.: Science **321**, 792 (2008)
4. Cohen, A.J., Mori-Sánchez, P., Yang, W.: Chem. Rev. **112**, 289 (2012)
5. Cramer, C.J., Truhlar, D.G.: Phys. Chem. Chem. Phys. **11**, 10757 (2009)
6. Seidl, M.: Phys. Rev. A **60**, 4387 (1999)
7. Seidl, M., Gori-Giorgi, P., Savin, A.: Phys. Rev. A **75**, 042511 (2007)
8. Gori-Giorgi, P., Vignale, G., Seidl, M.: J. Chem. Theory Comput. **5**, 743 (2009)
9. Buttazzo, G., De Pascale, L., Gori-Giorgi, P.: Phys. Rev. A **85**, 062502 (2012)
10. Hohenberg, P., Kohn, W.: Phys. Rev. **136**, B 864 (1964)
11. Levy, M.: Proc. Natl. Acad. Sci. USA **76**, 6062 (1979)
12. Langreth, D.C., Perdew, J.P.: Solid State Commun. **17**, 1425 (1975)
13. Gunnarsson, O., Lundqvist, B.I.: Phys. Rev. B **13**, 4274 (1976)
14. Seidl, M., Perdew, J.P., Levy, M.: Phys. Rev. A **59**, 51 (1999)
15. Seidl, M., Perdew, J.P., Kurth, S.: Phys. Rev. Lett. **84**, 5070 (2000)
16. Malet, F., Gori-Giorgi, P.: Phys. Rev. Lett. **109**, 246402 (2012)
17. Malet, F., Mirtschink, A., Cremon, J.C., Reimann, S.M., Gori-Giorgi, P.: Phys. Rev. B **87**, 115146 (2013)
18. Gori-Giorgi, P., Seidl, M., Vignale, G.: Phys. Rev. Lett. **103**, 166402 (2009)
19. Mirtschink, A., Seidl, M., Gori-Giorgi, P.: J. Chem. Theory Comput. **8**, 3097 (2012)
20. Casula, M., Sorella, S., Senatore, G.: Phys. Rev. B **74**, 245427 (2006)
21. Helbig, N., Fuks, J.I., Casula, M., Verstraete, M.J., Marques, M.A.L., Tokatly, I.V., Rubio, A.: Phys. Rev. A **83**, 032503 (2011)
22. Räsänen, E., Seidl, M., Gori-Giorgi, P.: Phys. Rev. B **83**, 195111 (2011)
23. Bednarek, S., Szafran, B., Chwiej, T., Adamowski, J.: Phys. Rev. B **68**, 045328 (2003)
24. Abedinpour, S.H., Polini, M., Xianlong, G., Tosi, M.P.: Eur. Phys. J. B **56**, 127 (2007)
25. Calmels, L., Gold, A.: Phys. Rev. B **56**, 1762 (1997)
26. Vieira, D., Capelle, K.: J. Chem. Theory Comput. **6**, 3319 (2010)
27. Vieira, D.: Phys. Rev. B **86**, 075132 (2012)
28. Buijse, M.A., Baerends, E.J., Snijders, J.G.: Phys. Rev. A **40**, 4190 (1989)
29. Helbig, N., Tokatly, I.V., Rubio, A.: J. Chem. Phys. **131**, 224105 (2009)

30. Wagner, L.O., Stoudenmire, E.M., Burke, K., White, S.R.: Phys. Chem. Chem. Phys. **14**, 8581 (2012)
31. Grüning, M., Gritsenko, O.V., Baerends, E.J.: J. Chem. Phys. **118**, 7183 (2003)
32. Stoudenmire, E., Wagner, L.O., White, S.R., Burke, K.: Phys. Rev. Lett. **109**, 056402 (2012)
33. Levy, M., Perdew, J.P.: Phys. Rev. A **32**, 2010 (1985)
34. Perdew, J.P., Tao, J., Staroverov, V.N., Scuseria, G.E.: J. Chem. Phys. **120**, 6898 (2004)
35. Tao, J., Perdew, J.P., Staroverov, V.N., Scuseria, G.E.: Phys. Rev. Lett. **91**, 146401 (2003)
36. Cotar, C., Friesecke, G., Klüppelberg, C.: Comm. Pure Appl. Math. **66**, 548 (2013)
37. Monge, G.: Mémoire sur la théorie des déblais et des remblais, Histoire Acad. Sciences, Paris (1781)
38. Kantorovich, L.V.: Dokl. Akad. Nauk. SSSR. **37**, 227 (1942)
39. Villani, C.: Topics in optimal transportation. Grad. Stud. Math., vol. 58. American Mathemaical Society, Providence, RI (2003)
40. Mendl, C.B., Lin, L.: Phys. Rev. B **87**, 125106 (2013)